*Desalination and Water Treatment*
www.deswater.com

doi: 10.1080/19443994.2014.981224

57 (2016) 3205–3217
February

Taylor & Francis
Taylor & Francis Group

# Reductive transformation and enhancement in biodegradability of mono-azo dye by high carbon iron filings (HCIF)

Raja Kumar*, Alok Sinha

*Department of Environmental Science & Engineering, Indian School of Mines, Dhanbad 826004, Jharkhand, India, Tel. +91 8986821608; email: raja.kumar1010@gmail.com (R. Kumar), Tel. +91 9471518560; email: aloksinha11@yahoo.com (A. Sinha)*

Received 22 April 2014; Accepted 18 October 2014

ABSTRACT

In the present study, reductive degradation of commercially used mono-azo dye, C.I. Acid Orange 7 (AO7), has been investigated using high carbon iron filings (HCIF) in batch reactors. Extent of dye degradation was monitored on the basis of removal efficiencies of various parameters like color and chemical oxygen demand (COD). Enhancement in biodegradability of AO7 dye was evaluated on the basis of an increase in $BOD_5$ and $BOD_5$/COD ratio. The effect of different operating conditions, namely, initial pH, HCIF dosage, and initial dye concentration, were evaluated at mixing intensity of 30 rpm for 120 min. More than 90% decolorization was achieved at all experimental conditions studied. Optimum decolorization efficiency of 99.55% was achieved at pH 3 using HCIF dosage of 28.56 g/l and 100 mg/l initial AO7 concentration. In the adsorption experiments carried out at different initial dye concentrations, a significant amount of unreduced dye remained adsorbed onto the HCIF even after 120 min of reaction time, thus, decreasing the actual reduction efficiency. Under the optimal reaction conditions, COD removal efficiency of 64.71% was observed. The biological oxygen demand (BOD) for 100 mg/l AO7 dye solution increased from 2.32 mg/l of the untreated dye solution to 27.84 mg/l after 120 min. Biodegradability measured as $BOD_5$/COD ratio was increased significantly from 0.0136 of the original solution to 0.464 after 120 min. First-order dye degradation kinetics was evaluated at different operating conditions. In experiments conducted at different pH, highest degradation constant ($k_{obs}$) of 1.40 $min^{-1}$ was recorded at pH 3. $k_{obs}$ increased linearly with increase in HCIF dosage whereas highest surface area normalized rate constant ($k_{SA}$) of 0.0495 l/m/ min was achieved at 28.56 g/l HCIF dosage. The $k_{obs}$ decreased as the initial AO7 concentration increased, suggesting saturation of ZVI surface reactive sites. The results suggest that HCIF can be used as a promising pre-treatment method, for recalcitrant azo dyes during conventional treatment methods.

*Keywords:* Azo dye; Acid Orange 7 (AO7); High carbon iron filings (HCIF); Reductive decolorization; Adsorption; Biodegradability

*Corresponding author.

## 1. Introduction

Textile industry is blamed for producing large volumes of colored effluent exiting mostly from spent dyebaths and dye rinsing operations. It is estimated that approximately 2% of the dyes produced is discharged directly in aqueous effluent and 10% is subsequently lost during the coloration process [1]. The most commonly used class of dyes for dyeing purpose is azo dyes. These are synthetic dyes bearing one or more N=N linkages. Their structural complexity confers their resistance to degradation by light, acid, bases, and oxygen, thus, making them dyers favorite [2]. Unfortunately, these properties of azo dyes accounts for their recalcitrance and resistance to conventional biological treatment process [3–5] which is considered as a cheapest wastewater treatment method. More than 53% of these commonly used azo dyes are identified as nonbiodegradable compounds and some are proven to be toxic and carcinogenic [6]. The discharge of such harmful organics into receiving water bodies poses a serious threat to the environment and warrants a need to contain them prior to their release.

Although environmental engineers are endeavoring hard to develop effective treatment strategies to degrade dye molecules, an ideal technology still remains to be proposed since both physical and chemical treatment processes have their own limitations of either efficiency or cost. Hence, it would be ideal to use a cheap and effective pretreatment technology that could break the azo linkage, followed by aerobic biological treatment to achieve complete mineralization of azo dyes.

Iron-based technology is seen as an effective treatment alternative for many environmental pollutants. Pure zero valent iron, cast iron filings, and the bimetals of iron have been used to treat a wide array of environmental pollutants. High carbon iron filings (HCIF) are iron/carbon/silicon alloys (2–4% C; 1–3% Si), in which more carbon is present that remains embedded as graphite flakes within the metal [7]. Lower cost (compared to conventional $Fe^0$), capability of reductive transformation of many chlorinated hydrocarbons [7–9], nitroaromatic compounds [10,11], explosives [12,13], heavy metals [14], and dyes [15] have made cast iron filings as a material of choice for environmental remediation.

Based on this promising technology, the main objective of this research is to investigate the decolorization of azo dye Acid Orange 7 (AO7) solutions by HCIF under varying experimental conditions such as pH, HCIF dosage, and different initial dye concentrations. Enhancement in biodegradability is evaluated by analyzing global parameters such as variation in biological oxygen demand ($BOD_5$) vs. time and the $BOD_5$/chemical oxygen demand (COD) ratio of the treated effluent vs. time to find the condition of full biodegradability. This ratio considers the most used parameter to quantify the biodegradability of a contaminated effluent. Hopefully, this work may provide a new insight into the treatability of industrial effluent using metals.

## 2. Materials and methods

### 2.1. Dye and chemicals

Commercially available mono-azo dye C.I. AO7 [4-(2-Hydroxy-1-naphthylazo) benzenesulfonic acid sodium salt] which is a widely used anionic mono-azo dye [16] was chosen as a model of the hydro soluble phenylazonaphthol dyes due to its resistance to biological degradation. AO7 was purchased from Atul Ltd. (India) and was used as received. A CHNOS analyzer (Vario EL, Elementar, Germany) was used to determine the % carbon content of the solid dye samples. Characteristics of AO7 dye used in this study are shown in Table 1. Methanol (used in the adsorption experiments) and other chemicals used for BOD analysis were purchased from Merck (India). 1-Amino-2-napthol was purchased from Sigma-Aldrich (Germany). All chemicals used were of analytical purity.

### 2.2. Preparation and characterization of HCIF

Commercially available cast iron rod was chipped on a lathe machine and then ground into iron filings in a dough-sized ball mill. The filings were sieved and those between 40 (425 μm) and 80 (212 μm) mesh sizes

Table 1
The properties of azo dye Acid Orange 7 (AO7) used in this study

| Dye name | Acid Orange 7 C.I. 15510 |
|---|---|
| Molecular formula | C16H11N2NaO4S |
| M.W | 350.32 |
| $\lambda_{max}$ | 484 nm |
| COD* | 170 mg/l |
| TOC* | 49.33 mg/l |
| BOD* | 2.32 mg/l |
| BOD/COD* | 0.01367 |
| % Carbon** | 45.66 |

*Values obtained after experimental analysis for 100 mg/l AO7 dye.
**Value obtained after CHNS analysis.

were retained for use. HCIF, thus produced, was washed 5–6 times with $N_2$-sparged 1 N HCl with periodic shaking. Then, it was rinsed 10–12 times with $N_2$-sparged deionized (Milli Q) water. The washed filings were rinsed twice with acetone to remove moisture. Again, it was rinsed twice with 95% pure ethanol and dried for 1 h. This treatment yielded black metallic filings with no visible rust on the surface. HCIF was stored in a vacuum desiccator until use in various experiments. Carbon content, BET surface area, and XRD analysis of HCIF samples were performed.

Carbon content (percent weight basis) of HCIF as determined by LECO induction furnace instrument (LECO Corporation, St. Joseph, USA) was found to be 3.05% by weight. Surface area of the treated filings was determined by BET ($N_2$) analysis using a BET surface area analyzer (NOVA 4000e, Quantachrome Instruments, USA) to be 1.4 $m^2/g$. X-ray diffraction (XRD) spectra of the pre-treated HCIF surface were obtained using Bruker D8 Discover diffractometer (Bruker Advanced X-ray Solutions, Germany) using Cu $K_\alpha$ radiation. XRD spectra (see Fig. 1) of HCIF surface showed prominent peaks conformable to metallic iron. None of the peaks could be ascribed to any iron oxide phases.

### 2.3. Experimental procedure

Time series batch experiments were carried out in 35 ml capacity glass vials with screw caps (Borosil, India). All dye solutions were prepared using deionized (Milli Q) water and all reagents utilized were of analytical purity. The pH of the system, initial dye concentration, and HCIF dosage was amended as per experimental need. The initial pH was adjusted to the desired levels using HCl (0.5 M) or NaOH (0.1 M). For proper mixing, the vials were placed on a test tube rotator (Rotospin, Tarsons, India) at 30 rpm. The temperature was 25 ± 2 ˚C for all experiments. The vials were removed from the rotator in duplicate along with a blank at specified times for sampling and analysis, and were put on a magnet to allow iron particles to settle down quickly. Supernatant samples were filtered through GF/C filter paper (1.2 μm nominal pore size, Whatman, Springfield Mill, England) and were used for color, COD, and BOD analysis. Blank experiments showed a negligible variation of study values from the initial. In the experiments using 1-Amino-2-napthol (1A2 N), 1-Amino-2-naphthol (50 mg/l) was added as a powder at the start of the preparation procedure along with AO7 dye solution and HCIF. Two separate sets of blanks for this experiment consisted of 1A2 N along with only HCIF and the other with 1A2 N along with dye solution only.

Adsorption experiments were carried out at different initial AO7 dye concentrations. Both aqueous and solid phases of AO7 concentration was determined in each vial withdrawn at definite time interval. For determining the solid phase concentration, the aqueous phase of the 35 ml vial was transferred to another vial. To the vial containing the solid phase, 5 ml methanol was added and the contents were vortex mixed for 5 min. The solvent along with desorbed dye was transferred to another vial. Again 5 ml of methanol was added to the solid phase and the contents were mixed for another 5 min to ensure desorption of any residual AO7. This solvent was also transferred to the same vial. This 10 ml of methanol collected was filtered through GF/C filter paper and both the aqueous phase and the adsorbed AO7 dye concentration were determined in UV–vis spectropho-

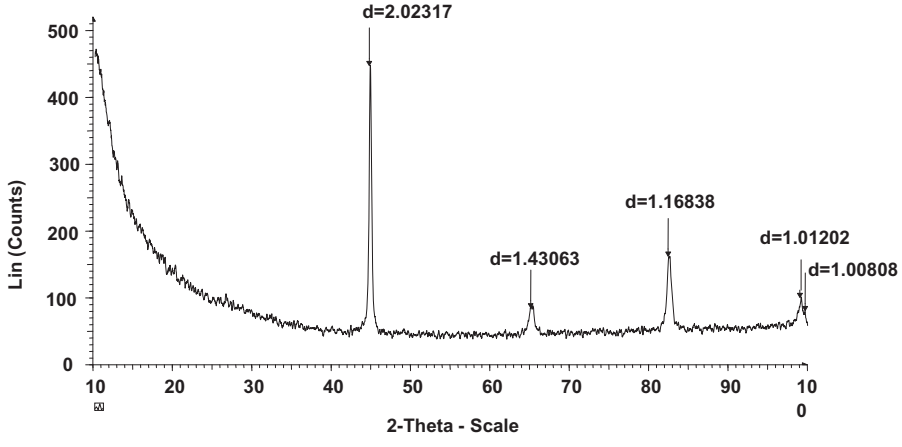


Fig. 1. XRD spectra of unrusted HCIF surface.

tometer using separate AO7 calibration curves made with deionized water and methanol, respectively.

### 2.4. Analytical procedure

$\lambda_{max}$ of AO7 was found at 484 nm using a UV–vis spectrophotometer (UV-1800 series, Shimadzu, Japan) and was used for quantification of dye in treated solution. UV–vis spectra of the dye solution were recorded from 200 to 600 nm after three times dilution of untreated and treated solution. Several sets of calibration curves were prepared under various pH conditions studied (i.e. pH 2, 3, 4, 5, 6, 7, 8, and 9) to reflect the variation of characteristic wavelength and absorbance, thereby avoiding expected error. To determine the change in the COD of reaction medium, initial COD of the untreated dye solution and that of a sample at different time intervals during the reaction were measured. COD of the samples were determined using Merck Spectroquant COD Cell test kit (Merck Millipore, Germany). Removal efficiencies of color and COD were also determined according to Eq. (1) mentioned below. The BOD of the samples was determined as described in standard methods [17]. Efficiency of HCIF for removal of color and COD was calculated using the following equation:

$$R\ (\%) = 100 \times (C_i - C_u)\ /C_i\ \% \quad (1)$$

where $R$ (%) = the removal efficiency, $C_i$ is the initial concentration (mg/l), and $C_u$ is the ultimate residual concentration (mg/l).

### 2.5. Kinetics analysis

The reductive decolorization of AO7 in a closed batch system can be summarily expressed as

$$nC + M \rightarrow \text{Acid Orange7 degradation byproducts} \quad (2)$$

The reaction kinetics can be evaluated by using Eq. (3) given below

$$\frac{dC}{dt} = -kMC^n \quad (3)$$

where $C$ is the AO7 concentration at time $t$, $M$ is the concentration of HCIF, and $n$ is the reaction order. Assuming that the initial HCIF concentration taken in each experiment did not change during the whole reaction; therefore, $kM = k_{obs}$ (observed rate constant in $min^{-1}$). Hence Eq. (3) becomes as

$$\frac{dC}{dt} = -k_{obs}C^n \quad (4)$$

Eq. (4) can be converted to Eq. (5) with the natural logarithm

$$\ln\left(-\frac{dC}{dt}\right) = n\ln C + \ln k_{obs} \quad (5)$$

Here, $dC/dt$ is negative since it is a loss process. Values of $n$ and $k_{obs}$ is determined from the plot of $\ln(-dC/dt)$ vs. lnC. It should be emphasized that $k_{obs}$ is not a true first order rate constant and is influenced by the surface area of HCIF accessible to AO7 dye molecules. Hence, the surface area normalized rate constant or specific reaction rate constant $k_{SA}$ ($l/m^2/min$) is determined to reflect the essential degradation ability of HCIF. The relationship between $k_{obs}$and $k_{SA}$ is shown in Eq. (6) below.

$$k_{obs} = k_{SA}\ \rho_a \quad (6)$$

where $\rho_a = a_s\ \rho_m$ is the surface area concentration of HCIF ($m^2/l$) of solution, $a_s$ is the specific surface area of the HCIF ($m^2/g$), and $\rho_m$ is the mass concentration of HCIF in solution (g/l). The values of reaction rate constants and specific rate constants for AO7 degradation reported by different researchers are shown in Table 2.

## 3. Results and discussion

### 3.1. Effect of initial pH

The actual dye containing wastewater has a wide range of pH values, so it is very necessary to investigate the influence of pH on decolorization process. When an effective collision between dye molecules and elemental iron happens, elemental iron as an electron donor loses electrons. Meanwhile, the dye molecule, as an electron acceptor, gets electrons, combines with $H^+$, turns into transitional products, and finally terminal products (see Fig. 2). As a consequence, the pH would strongly affect the degradation of AO7. It was anticipated that changes in pH will influence the decolorization of dye in two ways: (i) direct involvement of $H^+$ in the reaction at lower pH (ii) mass transport limitations imposed by the precipitation of a passive film on the metal surface at higher pH values [18]. The aqueous speciation of reducible contaminant and their reduced form and,

Table 2
Comparison of rates obtained in different studies using ZVI and Acid Orange 7

| Author | ZVI type | Sp. surface area (m2/g) | Dose (g/l) | Iron surface area (m2/l) | Dye conc. (mg/l) | pH | rpm | Reaction conditions | k (min−1) | kSA (l/m2 min) |
|---|---|---|---|---|---|---|---|---|---|---|
| Zhang et al. [23] | Amorphous (Fe, Si, and Fe–B alloy) | 15,000 mm2 | | 0.0833 | 100 | 6 | 200 | Aerobic/pH | 0.412 | 4.95 |
| | | | | 0.0556 | | 6 | | uncontrolled | 0.201 | 3.60 |
| | | | | 0.0278 | | 6 | | | 0.087 | 3.13 |
| | | | | 0.0833 | | 3 | | | 0.443 | 5.32 |
| | | | | 0.0833 | | 1 | | | 0.214 | 2.57 |
| Nam and Tratnyek [33] | Micron-sized pure iron | 0.0071 | 200 | 1.42 | 105 | 7 | 100 | Anaerobic/pH | 0.161 | 0.113 |
| | | | | | | | 120 | controlled | 0.245 | 0.173 |
| | | | | | | | 130 | | 0.306 | 0.215 |
| | | | | | | | 140 | | 0.380 | 0.268 |
| Bigg and Judd [37] | -do- | 0.5–1.0 | 23.15 | 3.94–23.15 | 7 | 5.8 | 800 | Anoxic/pH | 0.14 | |
| | | | | | | | 1,200 | controlled | 0.253 | |
| | | | | | | | 1,600 | | 0.30 | |
| | | | | | | | 2,000 | | 0.735 | |
| | | | 11.6 | | | | 2,000 | | 0.43 | |
| | | | 7.9 | | | | 2,000 | | 0.35 | |
| Mielczar-ski et al. [27] | -do- | 0.0051 | 8.2 | 0.041 | 35 | 2 | NA | Aerobic/pH | 0.006 | 0.156 |
| | | | | | | 3 | | controlled | 0.007 | 0.181 |
| Mu et al. [20] | Micron-sized pure iron | NA | 66.6 | NA | 100 | 3 | 120 | Aerobic/pH | 0.032 | |
| | | | | | | 4 | | uncontrolled | 0.018 | |
| | | | | | | 5 | | | 0.017 | |
| | | | | | | 6 | | | 0.016 | |
| | | | | | | 7 | | | 0.014 | |
| | | | | | 50 | 4 | | | 0.017 | |
| | | | | | 100 | | | | 0.018 | |
| | | | | | 150 | | | | 0.022 | |
| | | | | | 200 | | | | 0.020 | |
| | | | | | 250 | | | | 0.019 | |
| Hou et al. [38] | Micron-sized pure iron | 7.5 | 5 | 37.5 | 50 | 2 | NA | Anaerobic/ pH | 0.119 | 0.003 |
| | | | | | | 4 | | uncontrolled | 0.065 | 0.002 |
| | | | | | | 5 | | | 0.045 | 0.001 |
| | | | | | | 6 | | | 0.036 | 0.001 |
| | | | 5 | 37.5 | 50 | 4 | | | 0.0652 | 0.0017 |
| | | | | | 100 | | | | 0.0404 | 0.001 |
| | | | | | 200 | | | | 0.0333 | 0.0009 |
| | | | | | 300 | | | | 0.0293 | 0.0008 |
| | | | 1 | 7.5 | 50 | 4 | | | 0.0243 | 0.0032 |
| | | | 2 | 15 | | | | | 0.0441 | 0.0029 |
| | | | 4 | 30 | | | | | 0.0502 | 0.0017 |
| | | | 5 | 37.5 | | | | | 0.0652 | 0.0017 |
| This study | HCIF | 1.4 | 7.14 | 9.996 | 100 | 3 | 30 | Aerobic/pH | 0.474 | 0.0479 |
| | | | 14.28 | 19.992 | | | | uncontrolled | 0.802 | 0.0401 |
| | | | 28.56 | 39.998 | | | | | 1.981 | 0.0495 |
| | | | 42.84 | 59.99 | | | | | 2.801 | 0.0467 |
| | | | 57.12 | 79.996 | | | | | 2.817 | 0.0334 |
| | | | 28.56 | 39.998 | 100 | 2 | 30 | | 1.274 | 0.0318 |

(*Continued*)

Table 2 (*Continued*)

| Author | ZVI type | Sp. surface area (m2/g) | Dose (g/l) | Iron surface area (m2/l) | Dye conc. (mg/l) | pH | rpm | Reaction conditions | k (min−1) | kSA (l/m2 min) |
|---|---|---|---|---|---|---|---|---|---|---|
| | | | | | | 3 | | | 1.40 | 0.0350 |
| | | | | | | 4 | | | 1.264 | 0.0316 |
| | | | | | | 5 | | | 1.180 | 0.0295 |
| | | | | | | 6 | | | 0.690 | 0.0173 |
| | | | | | | 7 | | | 0.560 | 0.0140 |
| | | | | | | 8 | | | 0.593 | 0.0148 |
| | | | | | | 9 | | | 0.598 | 0.0150 |
| | | | 28.56 | 39.998 | 50 | 3 | 30 | | 3.955 | 0.0989 |
| | | | | | 100 | | | | 2.388 | 0.0597 |
| | | | | | 200 | | | | 2.308 | 0.0577 |
| | | | | | 300 | | | | 2.301 | 0.0575 |
| | | | | | 400 | | | | 2.269 | 0.0567 |
| | | | | | 500 | | | | 2.196 | 0.0549 |

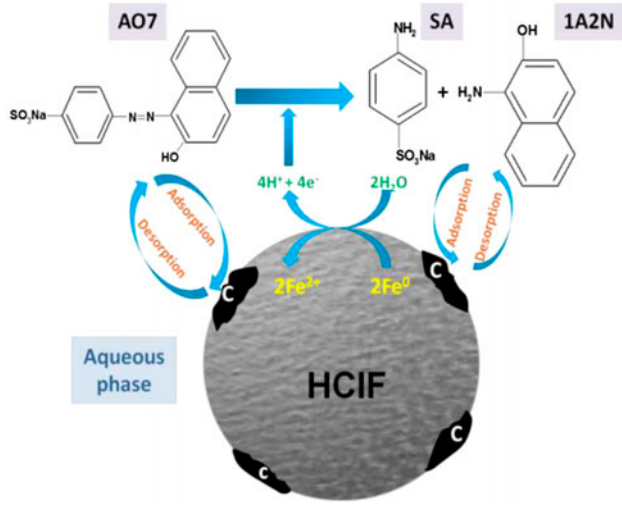


Fig. 2. Schematic representation of the interaction of AO7 with HCIF surface (abbreviations: C—Carbon; SA—Sulfanillic acid; 1A2N—1Amino-2-Napthol) (pathway adapted from Cao et al. [19]).

thus, their affinity to adsorptive surfaces is necessarily a pH-controlled phenomenon.

Effect of pH on the decolorization efficiency of AO7 was studied at different pH of solution ranging from pH 2 to 9 for 120 min reaction time. The results, as represented in Fig. 3, show that at all the initial solution, pH studied more than 90% decolorization of AO7 could be achieved within first 5 min of the reaction. Final AO7 color removal efficiencies recorded after 120 min were 99.52 ± 0.006 %, 99.55 ± 0.005%, 99.50 ± 0.015%, 99.42 ± 0.014%, 98.94 ± 0.038%, 98.56 ±

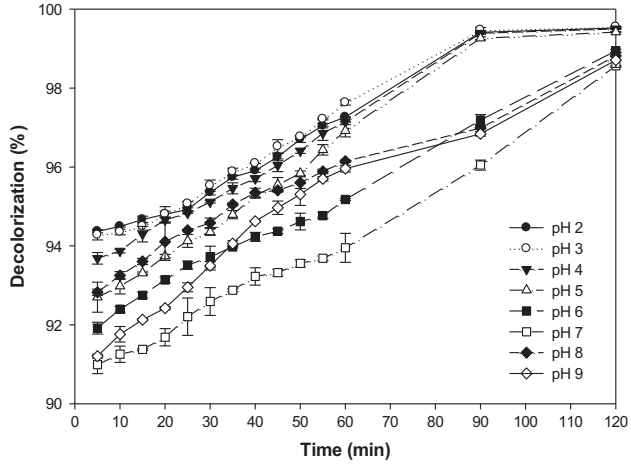


Fig. 3. Effect of different pH values on decolorization of Acid Orange 7 dye solution (initial conditions: HCIF dosage 28.56 g/l; dye conc. 100 mg/l; pH 2, 3, 4, 5, 6, 7, 8, and 9; mixing speed 30 rpm).

0.007%, 98.81 ± 0.092%, and 98.71 ± 0.18% for pH 2, 3, 4, 5, 6, 7, 8, and 9, respectively.

Highest decolorization efficiencies were observed at acidic pH (pH < 5). This variation can be ascribed to the fact that changes in solution pH affect the reduction potential of the reaction, $Fe^0 - 2e^- = Fe^{2+}$. With the increase in $H^+$ concentration, i.e. the decrease in pH, rapid corrosion of HCIF surface could occur. Consequently, the $Fe^{2+}$ concentration in the solution is increased. According to the Nernst equation, the reduction potential of reaction ($Fe^0 - 2e^- = Fe^{2+}$) is increased; hence, the efficiency of AO7 degradation increased as the solution pH decreased [20]. Researchers have also indicated that this aqueous $Fe^{2+}$ could be helpful in regenerating the otherwise passivated iron surface [21,22].

Maximum decolorization was observed at pH 3 instead of pH 2. This is possibly because of an acid-driven effect caused by excess HCl in solution. At lower pH, the surface of iron is positively charged which favors the adsorption of the dye molecules with negative charges (induced by sulfonate group present in them). Addition of excess HCl would lead excess $H^+$ to adsorb on the iron surface, which gains electrons from the iron to form $H_2$ bubbles. These $H_2$ bubbles tend to occupy the reactive sites, thus slowing down the decolorization process at strongly acidic conditions [23]. This could be the possible reason why decolorization efficiency, which was highest at pH 2 after first 5 min, retarded after 60 min of reaction time. Noubactep [24] and Zhang et al. [23] have also reported low decolorization efficiencies at lower acidic pH values using metallic iron.

Another inference drawn from the result suggests that acidic and alkaline pH favored dye decolorization, but the reaction was retarded in the neutral and weakly acidic solution. The literature reports that iron corrosion at pH > 4 is of "oxygen absorption" type, a mechanism controlled by the nature of the oxide-film (composition, porosity, thickness) on metal surfaces, and the rate of contaminant diffusion through this film [25]. When the solution pH is above the isoelectric point, i.e. $pH_{pzc} \approx 8$ (pzc stands for the point of zero charge), this oxide surface becomes negatively charged and the reactive sites on the HCIF surface could be easily blanketed by the corrosion products [26]. This blanket prevents the diffusion of azo dye molecules to the reactive sites on iron surface [27,28]. Hence, at alkaline pH (pH 8 and 9) dye might get removed from the aqueous phase by adsorption and/or co-precipitation, even if it is not reduced, regardless from the redox reactivity [24,29–31]. The corrosion of iron by water is slow at neutral pH [32]; hence, at pH 6 and 7, neither much of the rejuvenated iron surface and $H^+$ were present as in case of acidic conditions nor was the oxide and hydroxide coated adsorptive surface area as in case of alkaline conditions, hence, this could account for slower and lower decolorization. In general, this finding has a very practical meaning because dye removal reaction could be carried out using HCIF at all pH conditions continuously achieving around 95% efficiency that too without adding any acid or buffer.

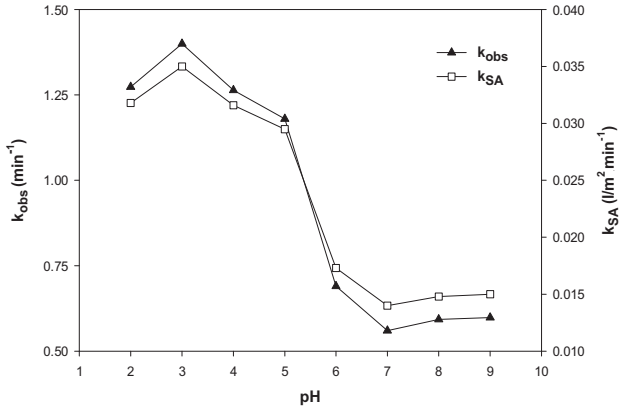


Fig. 4. Effect of pH on the observed rate constant and specific rate constant.

The kinetic results of decolorization of AO7 at different pH values are shown in Fig. 4. The highest $k_{obs}$ and the corresponding $k_{SA}$ value of 1.4 $min^{-1}$ and 0.035 $l/m^2/min$, respectively, were obtained at pH 3. The values of $k_{obs}$ evolved in this study are higher than those reported previously for the degradation of AO7 using iron metal. Depending upon the initial reaction conditions and low mixing intensity, the values of $k_{SA}$ obtained in this study are comparable to those listed in Table 2. Higher $k_{SA}$ value of 0.113 $l/m^2$ min by Nam and Tratnyek [33] using pure iron emphasizes upon the better contaminant removal ability of iron particles in anaerobic pH-controlled reaction conditions and at vigorous mixing intensities (see Table 2). However, practical applicability of iron particles for the treatment of textile wastewater lies in its efficiency to degrade dyes under aerobic condition with minimum energy investment. Besides, available literature reveals that at mixing rate greater than 40 $min^{-1}$, the iron corrosion process is accelerated which remains suspended in the system. Unreduced dye molecules gets entrapped in the matrix of iron oxides and co-precipitates [24].

### 3.2. Effect of initial HCIF dose

The effect of iron dosage on removal efficiencies is shown in Fig. 5. The results show 54.93 ± 1.11%, 75.13 ± 0.96%, 96.25 ± 0.38%, 96.79 ± 0.15%, and 96.91 ± 0.08%

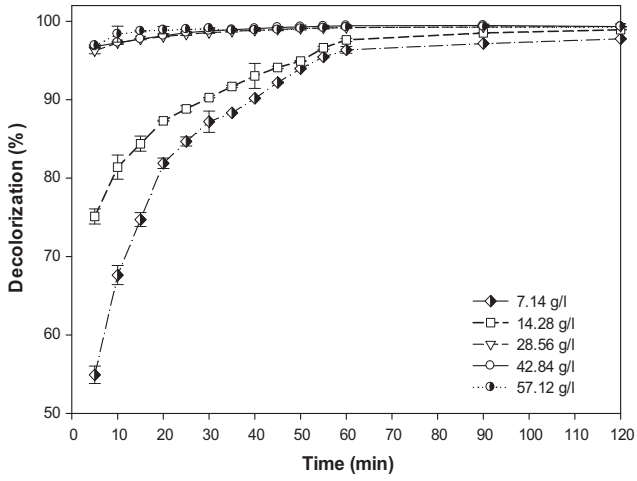


Fig. 5. Effect of different HCIF doses on decolorization of Acid Orange 7 dye solution (initial conditions: pH 3; dye conc. 100 mg/l; mixing speed 30 rpm).

decolorization efficiencies by HCIF doses of 7.14, 14.28, 28.56, 42.84, and 57.12 g/l, respectively, within first 5 min of treatment time. Increasing dosage of iron particles provides substantially more surface active sites to accelerate the initial reaction, resulting in more iron particles colliding with more azo dye molecules; hence, the color removal efficiencies improved with respect to the iron dosage during the initial reaction time. Over the course of 120 min, the color removal efficiencies were 97.76 ± 0.012%, 98.93 ± 0.02%, 99.34 ± 0.016%, 99.32 ± 0.01%, and 99.31 ± 0.01% for HCIF doses of 7.14, 14.28, 28.56, 42.84, and 57.12 g/l, respectively. The corresponding first-order kinetic constant ($k_{obs}$) increased linearly with increase in HCIF dosage (see Fig. 6). The value of $k_{obs}$ increased by over seven times with the increase in HCIF dosage from 7.14 g/l to 57.12 g/l and

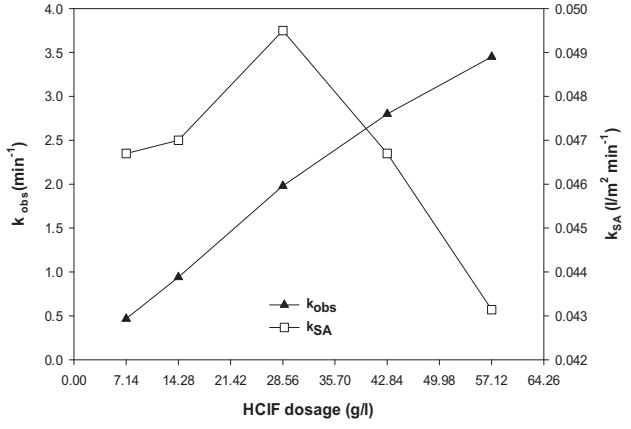


Fig. 6. Effect of HCIF dosage on the observed rate constant & specific rate constant.

was comparative with those reported by other researchers listed in Table 2. The observed variation in the corresponding specific rate constant ($k_{SA}$) was nonlinear and was recorded highest of 0.0495 l/m$^2$/min for 28.56 g/l iron dosage. It was also observed that value of $k_{SA}$ did not vary significantly after increasing the HCIF dosage beyond 28.56 g/l, suggesting that increasing the HCIF dosage for AO7 dye removal would be feasible only up to a certain point. At HCIF dosage of 28.56 g/l, dye removal reaches its optimum and with the increase in dosage, the removal efficiency decreases. This unusual precept can be attributed to the fact that the presence of excessive iron in the acidic solution system could be detrimental since the final pH of the system could reach higher values, thereby decreasing the degradation rate [34].

### 3.3. Effect of initial dye concentration

The effect of initial concentrations of AO7 on its decolorization efficiency were evaluated in a concentration range of 50–500 mg/l using optimum HCIF dosage of 28.56 g/l at pH 3. As shown in Fig. 7, the final decolorization efficiencies achieved after 120 min decreased nominally with increasing initial dye concentration, i.e. 99.86 ± 0.01%, 99.82 ± 0.05%, 99.76 ± 0.025%, 99.64 ± 0.056%, 99.54 ± 0.06%, and 99.50 ± 0.053% for initial dye concentrations of 50, 100, 200, 300, 400, and 500 mg/l, respectively. Even though the initial reaction was slow at higher dye concentrations, greater than 99.50% decolorization efficiency was achieved at all the initial dye concentrations studied. As the dye concentration is increased, the competition

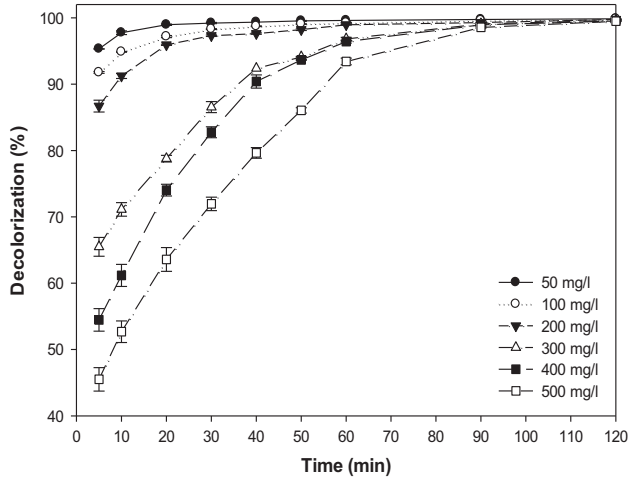


Fig. 7. Effect of different initial dye concentration on decolorization of AO7 dye solution (initial conditions: HCIF dosage = 28.56 g/l; pH 3, mixing speed 30 rpm).

between dye molecules to occupy the restricted number of reactive sites on iron surface is increased. The reactive sites may remain clogged by adsorbed dye molecules and their reduced byproducts. But as the reaction proceeds, simultaneous rejuvenation of iron surface and bubbling of the generated $H_2$ in the system (at low pH) may cause convection in the system. This prevents particle accumulation and keeps iron surfaces clean by removing the reduced alteration products from them [26,35]. This accounts for continuous and rapid adsorption and reduction of AO7 from aqueous solution, thus, revealing a strong degradation capacity of HCIF.

Fig. 8 shows the effect of varying initial AO7 dye concentration on the reduction kinetic constants. Highest value of $k_{obs}$ and $k_{SA}$ recorded was 3.955 $min^{-1}$ and 0.0989 $l/m^2/min$, respectively, for 50 mg/l initial dye concentration. With further increase in initial dye concentration, the values of kinetic parameters decreased very nominally. ZVI-mediated reaction is known to shift from first-order to zero-order kinetics depending on the initial contaminant concentration [33,36]. When the ratio of dye molecules to the available reactive sites on HCIF is low, competition between dye molecules to occupy the reactive sites is absent. Such circumstance results in first-order decolorization kinetics with respect to dye concentration. At high initial dye concentrations, when the ratio of dye molecules to the available reaction site is high, the competition between dye molecules to occupy the iron reactive sites increases. Consequently, the surface reactive sites get saturated and the decolorization rate becomes limited by availability of rejuvenated reactive sites and the kinetics shifts to zero order.

### 3.4. Adsorption of AO7 onto HCIF

The reductive degradation of compounds by HCIF is a heterogeneous or surface-mediated reaction. Such reactions require that the reactants reach the solid surface, where they can interact with reactive sites (i.e. iron) or nonreactive sites (i.e. graphite). Chemical reactions involving the breaking of bonds occurs at the reactive sites and nondestructive sorption occurs at the nonreactive sites [8,9]. Although, it has been demonstrated that exposed graphite can also mediate reduction of contaminants by conducting electron and atomic hydrogen generated during iron corrosion [39]. Hence, experiments were carried out to find the amount of dye adsorbed onto the HCIF surface at varying initial dye concentration. Fig. 9 shows the time course variation in the percentage of AO7 adsorbed onto the HCIF surface at different initial dye concentrations studied. The highest amount of adsorbed AO7 dye could be recovered in samples withdrawn after 5 min for all initial dye concentrations studied. After 120 min, the percentage of dye remaining adsorbed was 1.33, 1.76, 1.99, 4.23, 6.04, and 8.3% for 50, 100, 200, 300, 400, and 500 mg/l initial dye concentrations, respectively. It means that although more than 99.50% of AO7 was decolorized by HCIF at all initial dye concentrations, some of it still remains unreduced. This could be because of dye molecules remaining diffused into the intra-particle pores on the graphite surface [40]. Thus, the proper characterization of dye reduction in the HCIF surface in this system may require correction for the initial loss to nonreactive sites. Hence, if we go on to calculate the actual reduction efficiency the formula would be

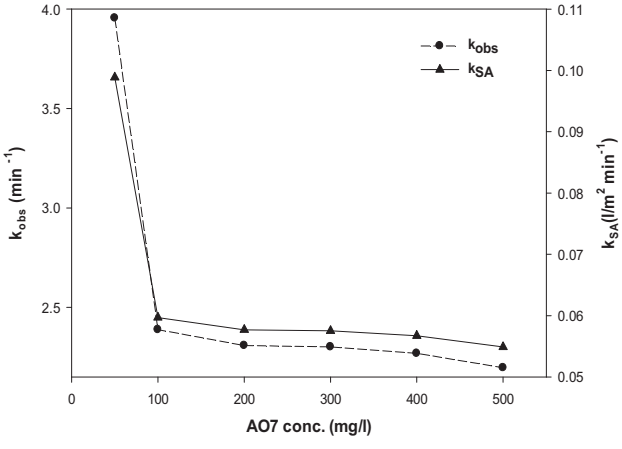


Fig. 8. Effect of initial AO7 concentration on the observed rate constant and specific rate constant.

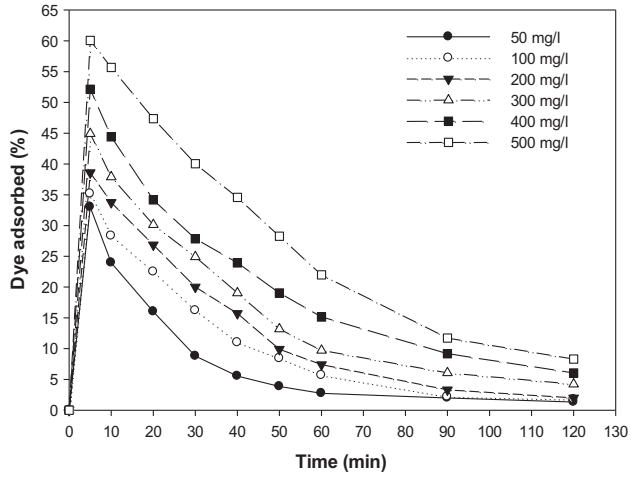


Fig. 9. Adsorption of AO7 onto HCIF at different initial dye concentrations.

$$RE(\%) = 100 \times [C_i - (C_a + C_s)]/C_i \ \% \quad (7)$$

where $RE$ (%) = the AO7 reduction efficiency, $C_i$ is the initial AO7 concentration (mg/l), $C_a$ is the aqueous AO7 concentration (mg/l), and $C_s$ is the concentration of AO7 adsorbed onto HCIF. From Eq. (2), the reduction efficiencies of AO7 would be 98.53, 98.27, 96.82, 96.52, and 96.18% for 50, 100, 200, 300, 400, and 500 mg/l initial dye concentrations, respectively.

The surface area of HCIF was found to be 1.4 $m^2/g$. The cross-sectional area of the AO7 is on the order of 1.3 $nm^2$ per molecule [41]. Hence, with initial dye concentration of 100 mg/l, the number of molecules present in the system is $6.02 \times 10^{18}$ molecules. Assuming a constant monolayer surface coverage of AO7 molecules onto the HCIF, it results that $1.08 \times 10^{18}$ molecules could be adsorbed to the surface which is 18% of that present in the system. But, the adsorption efficiency experimentally achieved in the first 5 min for the same initial dye concentration is 35%, illustrating a vertical configuration of the assembly of adsorbed molecules. From the adsorption data, the value of saturation capacity in μmoles of AO7 per $m^2$ ($\alpha$), as determined from the Langmuir isotherm equation for each dye concentration, was found to increase with ascending initial AO7 concentrations. Comparing the $\alpha$ values as a function of initial AO7 concentration yields a Langmuir-like trend (see Fig. 10), according to which,

$$\alpha = (C_{max} bc)/(1 + bc) \quad (8)$$

The maximum saturation value, $C_{max}$, determined from nonlinear regression was found to be 68 μmol/$m^2$, corresponding to about 41 molecules per square nm of HCIF surface. This value supports the experimental claim that the dye molecules could remain densely adsorbed in a layered vertical configuration. Similar, densely packed nonflat arrangement of AO7 molecules onto n-ZVI have also been reported by Freyria et al. [41].

### 3.5. UV–vis spectral study of degradation mechanism

Different structural units and groups in a dye molecule exhibit different absorbance peaks. The UV–vis spectra of AO7 scanned over the wavelength range of 200–600 nm at different reaction times is shown in Fig. 11. AO7 is characterized by one main band in the visible region, with its maximum absorption at 484 nm and two bands in the ultraviolet region located at 227 nm and 310 nm. These observed peaks correspond to chromophore containing azo linkage, benzene ring, and naphthalene ring, respectively [42]. Strong absorbance band at 484 nm is due to $n$–$\pi^*$ transition of azo bonds and other bands at 227 and 310 nm, and a doublet at 262 and 255 nm were due to $\pi$–$\pi^*$ transition of aromatic rings of AO7 molecule [27,38]. During the dye decolorization process, the intensity of bands at 227, 310, and 484 nm became very weak after 5 min of reaction and completely disappeared thereafter. New band at 250 nm appeared in all the spectra recorded indicating the formation of substituted aromatic amines [33]. Since both the byproducts of AO7 degradation bear amino group (–$NH_2$) which is an auxochrome, it causes the wavelength shift to the longer area [19].

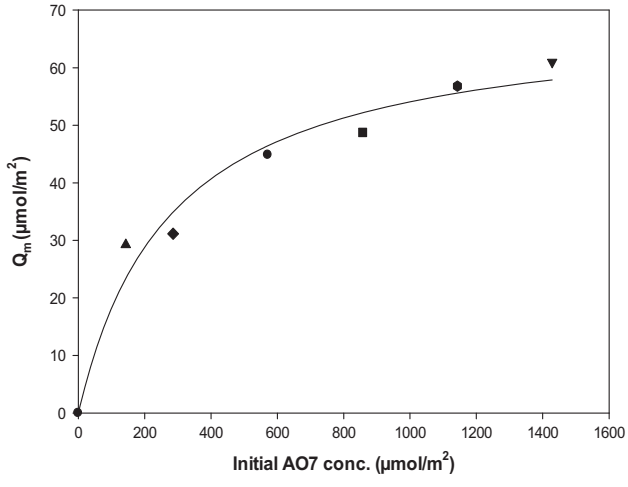


Fig. 10. Adsorption isotherm of AO7 as computed from data in Fig. 9.

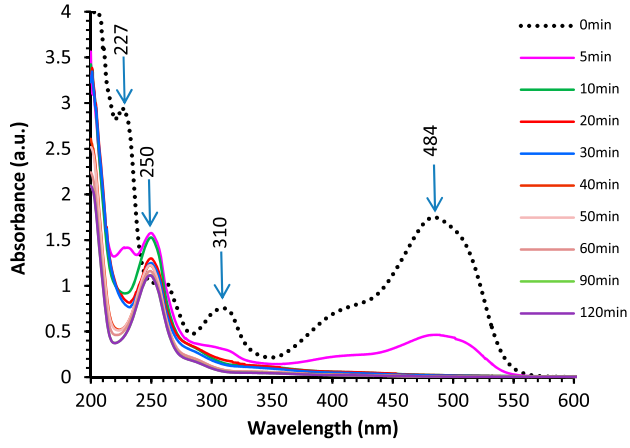


Fig. 11. UV–vis spectra of dye solution as a function of reaction time (initial conditions: pH 3; dye conc. 100 mg/l; HCIF dose 28.56 g/l; mixing speed 30 rpm).

### 3.6. Autocatalytic role of product amine

The byproducts of AO7 dye reduction were identified and quantified by HPLC and LCMS (data not shown). Reduction of AO7 molecule yields sulfanilic acid and 1-Amino-2-naphthol (Fig. 2). 1-Amino-2-naphthol (1A2 N) reportedly possesses redox-mediating properties and induces autocatalysis during AO7 dye reduction [43]. To test the effect of this phenomenon in context of HCIF-induced reductive decolorization, experiments were carried out using 1-Amino-2-napthol and AO7 dye. The results (data not shown) exhibit no influence of 1A2 N on the rates of AO7 reduction. In the vials consisting of 1A2 N and HCIF, autooxidation of 1A2 N was not observed in comparing the UV–vis spectra of HCIF-treated 1A2 N solution with that of unoxidized and fully oxidized 1A2 N solutions. In the other vials consisting of AO7 and 1A2 N, a very slow reduction of AO7 was observed. These results indicate towards negligible autocatalytic effect of 1A2 N in the highly reducing conditions of HCIF batch reactors, and the AO7 decolorization rates are governed predominantly by rapid HCIF-catalyzed reduction.

### 3.7 $BOD_5$ analysis and enhancement in biodegradability

Fig. 12 shows the increase in $BOD_5$ and $BOD_5$/COD ratio in 120 min reaction time. The initial $BOD_5$ of the untreated dye solution was very low (2.32 mg/l). Low $BOD_5$ value indicates that raw AO7 effluent inhibits the respiratory activity of bacterial seed. Therefore, besides being difficult to biodegrade, dye containing-effluent can also decrease the efficiency of biological treatment. The $BOD_5$ level gradually increased to 27.84 mg/l in 90 min-treated sample and remained stable hereafter. Improved $BOD_5$ results after reductive treatment by HCIF supports the fact that the structural stability of AO7 molecule conferred by –N=N– linkages accounts for its biorecalcitrance. Byproducts released after reductive cleavage of AO7 molecule could be easily utilized by microorganisms as food.

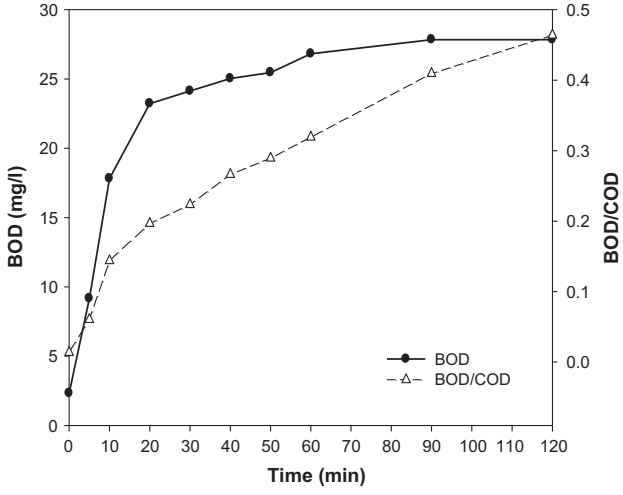


Fig. 12. Variation of BOD5 and BOD5/COD ratio with time (initial conditions: pH 3; AO7 conc. 100 mg/l; HCIF dose 28.56 g/l; mixing speed 30 rpm).

The biodegradability of wastewater is related to the ratio of $BOD_5$/COD. A $BOD_5$/COD ratio of 0.4 is generally considered as the cut-off point between biodegradable and difficult to biodegrade wastewater [44]. Domestic wastewater typically has a $BOD_5$/COD ratio between 0.4 and 0.8 [45]. For an untreated dye solution with initial COD concentration of 170 mg/l, the $BOD_5$/COD ratio was 0.0136 indicating its poor aerobic biodegradability. After 120 min of reductive treatment, as 64.71% of COD was removed, the $BOD_5$/COD ratio increased to 0.464, thus exceeding the quantitative index for organic matter biodegradability. $BOD_5$ is negatively correlated to COD (Pearson coefficient: –0.9369), i.e. decrease in the concentration of the recalcitrant proportion of COD enhances the biodegradability of the effluent.

## 4. Conclusions

This study reveals the strong dye degradation capability of HCIF. Optimal experimental conditions for decolorization and reductive degradation of azo dye AO7 were established. HCIF was found to be capable of removing more than 98% of color at all pH examined, thus, eliminating the need of adjusting pH of azo dye wastewater before treatment. However, optimum decolorization efficiencies were achieved at acidic pH. More than 50% decolorization was achieved at all HCIF dosages within 5 min and the efficiencies exceeded 95% at all dosages within 120 min. The optimum dosage of 28.56 g/l showed 99.34% decolorization efficiency at the end of the experiment. COD removal efficiency of 64.71% was achieved after 120 min of reaction time. Significantly, better aerobic biodegradability properties of the treated AO7 solution were obtained after 120 min with $BOD_5$/COD ratio increasing from 0.0136 to 0.464.

Kinetics analysis reveals that highest first-order degradation rate constants were highest at acidic pH and lowest at neutral, circumneutral, and basic pH conditions. The observed degradation rate constants at different HCIF dosages increased linearly with the increase in dosage, but the surface area normalized rate constant was highest at 28.56 g/l HCIF dosage. With respect to the initial dye concentration, the

degradation constant decreased with increase in AO7 concentration. The degradation kinetics tends to shift to zero-order kinetics at higher dye concentrations, suggesting that the reaction at the surface is the rate-determining step. High adsorption efficiency exhibited in first 5 min denotes vertically stacked assembly of dye molecules onto the HCIF surface. During the decolorization process, adsorption, reduction and catalysis steps occur on the HCIF surface. By virtue of these surface phenomena, HCIF can reduce the risk associated with the passing of target pollutants untreated through a treatment system; thus, beside being lower in cost, it enjoys an another edge over conventional $Fe^0$.

In summary, HCIF can quickly decolorize the colored wastewater via reductive cleavage of azo linkage of the conjugated system of the dye molecule. However, more information is needed for reducing the operating cost and evaluating the toxicity of the final treated wastewater before HCIF can be employed as a practical method for *in situ* wastewater treatment. It can be suggested that the combination of HCIF with aerobic biological treatment method can help achieving complete mineralization and detoxification of textile wastewater.

## Acknowledgments

The authors heartily acknowledge Technical Education Quality Improvement Program Phase II (TEQIP II), ISM, Dhanbad, for providing all necessary assistance for completion of this research work.

## References

[1] J.R. Easton, The problem of colour, in: P. Cooper (Ed.), Color In Dye House Effluent, Society of Dyers and Colourists, Bradford, 1995, pp. 9–21.
[2] H.Y. Shu, M.C. Chang, Decolorization effects of six azo dyes by $O_3$, $UV/O_3$ and $UV/H_2O_2$ processes, Dyes Pigm. 65 (2005) 25–31.
[3] I.M. Banat, P. Nigam, D. Singh, R. Marchant, Microbial decolorization of textile-dyecontaining effluents: A review, Bioresour. Technol. 58 (1996) 217–227.
[4] E. Razo-Flores, M. Luijten, B. Donlon, G. Lettinga, J. Field, Biodegradation of selected azo dyes under methanogenic conditions, Water Sci. Technol. 36 (1997) 65–72.
[5] T. Robinson, G. McMullan, R. Marchant, P. Nigam, Remediation of dyes in textile effluent: A critical review on current treatment technologies with a proposed alternative, Bioresour. Technol. 77 (2001) 247–255.
[6] W.J. Epolito, Y.H. Lee, L.A. Bottomley, S.G. Pavlostathis, Characterization of the textile anthraquinone dye Reactive blue 4, Dyes Pigm. 67 (2005) 935–946.
[7] D.R. Burris, T.J. Campbell, V.S. Manoranjan, Sorption of trichloroethylene and tetrachloroethylene in a batch reactive metallic iron-water system, Environ. Sci. Technol. 29 (1995) 2850–2855.
[8] A. Sinha, P. Bose, Interaction of 2-chloronaphthalene with high carbon iron filings (HCIF): Adsorption, dehalogenation and mass transfer limitations, J. Colloid Interface Sci. 314 (2007) 552–561.
[9] A. Sinha, P. Bose, Interaction of 2,4,6-trichlorophenol with high carbon iron filings: Reaction and sorption mechanisms, J. Hazard. Mater. 164 (2009) 301–309.
[10] J.M. Thomas, R. Hernandez, C.-H. Kuo, Single-step treatment of 2,4-dinitrotoluene via zero-valent metal reduction and chemical oxidation, J. Hazard. Mater. 155 (2008) 193–198.
[11] J. Dong, Y. Zhao, R. Zhao, R. Zhou, Effects of pH and particle size on kinetics of nitrobenzene reduction by zero-valent iron, J. Environ. Sci. 22 (2010) 1741–1747.
[12] S.Y. Oh, P.C. Chiu, B.J. Kim, D.K. Cha, Enhancing Fenton oxidation of TNT and RDX through pretreatment with zero-valent iron, Water Res. 37 (2003) 4275–4283.
[13] S.Y. Oh, D.K. Cha, B.J. Kim, P.C. Chiu, Reductive transformation of hexahydro-1,3,5-trinitro-1,3,5-triazine, octahydro-1,3,5,7-tetranitro-1,3,5,7-tetrazocine, and methylenedinitramine with elemental iron, Environ. Toxicol. Chem. 24 (2005) 2812–2819.
[14] C. Wanner, U. Eggenberger, V. Mäder, Reactive transport modelling of Cr(VI) treatment by cast iron under fast flow conditions, Appl. Geochem. 26 (2011) 1513–1523.
[15] Z. Shen, J. Shen, The use of ultrasound to enhance the degradation of the basic green by cast iron, J. Environ. Sci. 18 (2006) 1–3.
[16] H. Zollinger (Ed.), Color Chemistry: Synthesis, Properties and Applications of Organic Dyes and Pigments, second revised ed., VCH, Weinheim, 1991.
[17] APHA, Standard Method for the Examination of Water and Wastewater, twentieeth ed., APHA-AWWA-WPCF, Washington, DC, 2005.
[18] S. Chatterjee, S.R. Lim, S.H. Woo, Removal of reactive black 5 by zero-valent iron modified with various surfactants, Chem. Eng. J. 160 (2010) 27–32.
[19] J. Cao, L. Wei, Q. Huang, L. Wang, S. Han, Reducing degradation of azo dye by zero-valent iron in aqueous solution, Chemosphere 38 (1999) 565–571.
[20] Y. Mu, H.-Q. Yu, S. Zhang, J.-C. Zheng, Kinetics of reductive degradation of Orange II in aqueous solution by zero-valent iron, J. Chem. Technol. Biotechnol. 79 (2004) 1429–1431.
[21] Y.H. Huang, T.C. Zhang, Effects of dissolved oxygen on formation of corrosion products and concomitant oxygen and nitrate reduction in zero-valent iron systems with or without aqueous $Fe^{2+}$, Water Res. 39 (2005) 1751–1760.
[22] D. Mishra, J. Farrell, Understanding nitrate reactions with zero-valent iron using Tafel analysis and electrochemical impedance spectroscopy, Environ. Sci. Technol. 39 (2005) 645–650.
[23] C. Zhang, Z. Zhu, H. Zhang, Z. Hu, Rapid decolorization of Acid Orange II aqueous solution by amorphous zero-valent iron, J. Environ. Sci. 24 (2012) 1021–1026.

[24] C. Noubactep, An analysis of the evolution of reactive species in $Fe_0/H_2O$ systems, J. Hazard. Mater. 168 (2009) 1626–1631.
[25] C. Noubactep, Comments on "The effect of substituent groups on the reductive degradation of azo dyes by zerovalent iron" by M. Hou et al. [J. Hazard. Mater. 145 (2007) 305], J. Hazard. Mater. 148 (2007) 773–774.
[26] J. Fan, Y. Guo, J. Wang, M. Fan, Rapid decolorization of azo dye methyl orange in aqueous solution by nanoscale zerovalent iron particles, J. Hazard. Mater. 166 (2009) 904–910.
[27] J.A. Mielczarski, G.M. Atenas, E. Mielczarski, Role of iron surface oxidation layers in decomposition of azo-dye water pollutants in weak acidic solutions, Appl. Catal. B 56 (2005) 289–303.
[28] H. Zhang, L. Duan, Y. Zhang, F. Wu, The use of ultrasound to enhance the decolorization of the C.I. Acid Orange 7 by zero-valent iron, Dyes Pigm. 65 (2005) 39–43.
[29] E. Tipping, Some aspects of the interactions between particulate oxides and aquatic humic substances, Mar. Chem. 18 (1986) 161–169.
[30] R.J. Crawford, I.H. Harding, D.E. Mainwaring, Adsorption and coprecipitation of single heavy metal ions onto the hydrated oxides of iron and chromium, Langmuir 9 (1993) 3050–3056.
[31] K. Satoh, K. Kikuchi, S. Kinoshita, H. Sasaki, Potential capacity of co-precipitation of dissolved organic carbon (DOC) with iron(III) precipitates, Limnology 7 (2006) 231–235.
[32] T.L. Johnson, P.G. Tratnyek, Dechlorination of carbon tetrachloride by iron metal: The role of competing corrosion reactions, Am. Chem. Soc. 35 (1995) 699–701. Preprint extended abstract, Division of Environmental Chemistry, Anaheim, CA.
[33] S. Nam, P.G. Tratnyek, Reduction of azo dyes with zero valent iron, Water Res. 34 (2000) 1837–1845.
[34] L. Gomathi Devi, S. Girish Kumar, K. Mohan Reddy, C. Munikrishnappa, Photo degradation of methyl orange an azo dye by advanced Fenton process using zero valent metallic iron: Influence of various reaction parameters and its degradation mechanism, J. Hazard. Mater. 164 (2009) 459–467.
[35] E.J. Reardon, R. Fagan, J.L. Vogan, A. Przepiora, Anaerobic corrosion reaction kinetics of nanosized iron, Environ. Sci. Technol. 42 (2008) 2420–2425.
[36] W.J. Epolito, H. Yang, L.A. Bottomley, S.G. Pavlostathis, Kinetics of zero-valent iron reductive transformation of the anthraquinone dye Reactive Blue 4, J. Hazard. Mater. 160 (2008) 594–600.
[37] T. Bigg, S.J. Judd, Kinetics of reductive degradation of azo dye by zero-valent iron, Process Saf. Environ. Prot. 79 (2001) 297–303.
[38] M.F. Hou, F.B. Li, X.M. Liu, X.G. Wang, H.F. Wan, The effect of substituent groups on the reductive degradation of azo dyes by zerovalent iron, J. Hazard. Mater. 145 (2007) 305–314.
[39] S.Y. Oh, D.K. Cha, P.C. Chiu, Graphite-mediated reduction of 2,4-dinitrotoluene with elemental iron, Environ. Sci. Technol. 36 (2002) 2178–2184.
[40] D.R. Burris, R.M. Allen-King, V.S. Manoranjan, T.J. Campbell, G.A. Loraine, B. Deng, Chlorinated ethene reduction by cast iron: Sorption and mass transfer, J. Environ. Eng. 124 (1998) 1012–1019.
[41] F.S. Freyria, B. Bonelli, R. Sethi, M. Armandi, E. Belluso, E. Garrone, Reactions of acid Orange 7 with iron nanoparticles in aqueous solutions, J. Phys. Chem., C 115 (2011) 24143–24152.
[42] J. Yang (Ed.), Analysis of Dye, Chemical Industry Press, Beijing, 1987, pp. 156–163.
[43] F.P. Van der Zee, G. Lettinga, J.A. Field, The role of (auto)catalysis in the mechanism of an anaerobic azo reduction, Water Sci. Technol. 42 (2000) 301–308.
[44] J. Scott, D. Ollis, Integration of chemical and biological oxidation processes for water treatment II: Recent illustrations and experiences, J. Adv. Oxid. Technol. 2 (1997) 374–381.
[45] Metcalf and Eddy, Wastewater Engineering—Treatment, Disposal, and Reuse, International ed., McGraw-Hill, New York, NY, 1991.